Development and Characterization of Zinc Dry Electrodes for Wearable Electrophysiology

Cassia Rizq[1,2] and Alessandro D'Amico[2,3*]
Aidan Truel[2,3] and Joelle Faybishenko[2,3]
Min Suk Lee[1]
Jeong-Hoon Kim[1,4]
Gert Cauwenberghs[1] and Virginia R. de Sa[2,3]
[1]*Department of Bioengineering,* [2]*Department of Cognitive Science,*
[3]*Halıcıoğlu Data Science Institute,* [4]*Department of Electrical and Computer Engineering*
University of California, San Diego
La Jolla, USA

***Abstract*—Zinc dry electrodes were fabricated and investigated for wearable electrophysiology recording. Results from electrochemical impedance spectroscopy and electromyography functionality testing show that zinc electrodes are suitable for use in electrophysiology. Two electrode configurations were tested: a standard disc and a custom tripolar concentric ring configuration. However, no functional benefit was observed with the tripolar concentric ring electrodes as compared to the disc electrodes.**

***Index Terms*—Zinc, Electrodes, Concentric Ring Electrodes, EMG, Biosensing**

I. Introduction

With greater demand for wearable electrophysiology sensors, there has been great progress in the development of low-cost sensors. However, there is still a strong need for low-cost, high-quality electrodes, especially in no-gel (dry) contexts. Silver-Silver Chloride (Ag/AgCl) is considered state of the art for surface electrodes as silver is a slightly soluble salt capable of quickly saturating and coming to equilibrium [3]. As an accessible metal even less soluble than silver, zinc is a promising choice of electrode material. However, to our knowledge it has not been used in electrophysiology. Zinc electrodes were fabricated in two configurations (simple disc, and concentric ring) and tested alongside consistently fabricated stainless steel electrodes, to act as a control. Two methods were performed to evaluate the viability of zinc as an electrode for electrophysiological recordings: electrochemical impedance spectroscopy (EIS) and on-body electromyography (EMG). EIS was conducted to compare characteristic properties of zinc with those of Ag/AgCl and stainless steel. EMG data were collected from the fabricated zinc and stainless steel electrodes to test for signal quality and evaluate the functionality of zinc for wearable electrophysiology.

II. Methods

A. Electrode Fabrication

Both disc and concentric ring stainless steel electrodes were fabricated using a fablight FL4500 laser cutter on a 0.027" thick sheet of stainless steel purchased from Industrial Metal Supply. The zinc disc electrodes were fabricated using a belt sander on post-1982 pennies. The zinc concentric ring electrodes were manufactured on a Tormach 1100MX CNC machine with a sheet of 0.027" pure zinc purchased from McMaster-Carr. Once both types of concentric ring electrode were cut, DuPont connectors were crimped onto the ends of each lead to allow for connection during functionality testing, and heat shrink was applied to the exposed wires to prevent excess surface area exposure. For all electrodes undergoing EIS, the non-recording surface was coated in hot-melt adhesive manufactured by Surebonder. The disc electrodes had a notch removed in the hot-melt adhesive to allow for proper contact between the electrode and recording clip during EIS. The entire exposed surface of the concentric ring electrodes were submerged, while the discs were only partially submerged. Only the area of the submerged electrodes was used for the area-corrected EIS plots (see Figure 3). The electrode fabrication results are shown in Figure 1.

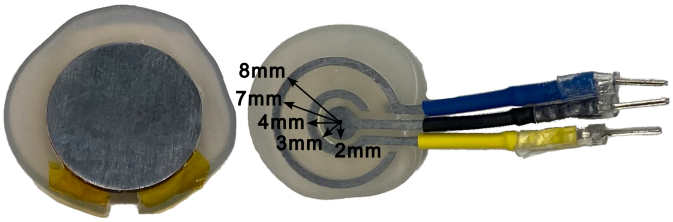

Fig. 1. Results of electrode fabrication. Shown are the zinc disc (left) and zinc concentric ring electrode (right). Steel versions were also fabricated and looked similar. Electrode backs were coated in hot melt adhesive to control skin contact area. Each number on the concentric ring electrode denotes the length of the segment from the origin to the arrow. The flat disc electrodes had an exposed surface area of 283.5 mm^2, while the concentric ring electrodes had an exposed surface area of 106.4 mm^2.

B. EIS Data

In order to characterize and compare the electrodes, EIS was performed on each electrode type. The EIS setup included a working, reference, and counter electrode, each connected to

*Corresponding author email: adamico@ucsd.edu

one lead from a PalmSens4 and arranged according to Figure 3. Galvanostatic impedance spectroscopy was performed using the compatible company software PSTrace v5.8 [8] with the following settings: pretreatment range of 100 pA to 100 μA, applied current range at 100 μA, fixed scan type, initial DC at 0.0, initial AC at 0.01, frequency type scan. Three trials were conducted for each fabricated electrode type. Impedance and negative phase data were exported to a comma separated file, where Excel was used to calculate the averages and standard deviations of the recordings across trials then plotted in Python as a solid line and shaded bar, respectively (see Figure 3). Additionally, the impedance data were normalized with respect to area where each of the data points were individually multiplied by the area then processed utilizing the same pipeline and plotting procedure.

The EIS results from all four electrodes were plotted alongside the EIS results of the Ag/AgCl electrodes fabricated utilizing ink, bleach, and electroplating from Lee et al. [5] to allow for comparison to the widely accepted Ag/AgCl electrode type for electrophysiological research purposes.

C. EMG Recordings

All EMG data were recorded simultaneously from a 22-year-old consented male. The study was approved by the University of California, San Diego's Institutional Review Board. All electrodes were in dry contact with the skin and held in place by medical tape. For both zinc and stainless steel, two sets of tripolar concentric ring electrodes were placed on the participant's right forearm, with one set closer to the hand and another closer to the elbow (referred to as hand and elbow, respectively). The back of the neck was used as the online reference and a forehead electrode roughly at FPz was used for ground. Data were re-referenced for offline analysis. The EMG data were amplified and digitized at 500 Hz by the BrainVision BrainAmp [1], and LabStreamingLayer [4, LSL] streams were created with the BrainAmp connector [2]. Visual stimuli were presented using the .NET build of the Godot Game Engine, version 4.1.3 [6], and LSL markers were sent at each onset. LSL streams were integrated using LabRecorder [9]. For the task, visual cues instructed the participant to relax, before being presented one of four gestures (clench, up, down, or expand) in a randomized order. For each movement, the participant was instructed to hold for the duration of the visual cue (200 ms). For offline analysis, the elbow inner disc electrodes were referenced to the hand inner disc electrodes. The tripolar Laplacian was also computed for the sets of hand and elbow electrodes [11] using:

$$L_{TP} = \frac{1}{3r^2}(16(V_M - V_D) - (V_O - V_D)) \tag{1}$$

where V_O, V_M, and V_D are the potentials measured from the outer ring, middle ring, and inner disc, respectively, and r is the distance from the center of the disc to the middle ring.
Data were band-pass filtered from 10 to 50 Hz with a 501-tap, non-causal, FIR Hamming window filter using SciPy [10]. Since there was added noise throughout the recording from unshielded wires, higher frequency data were not analyzed. The data were then epoched to the onset of the movement instruction cue starting 200 ms prior to the cue through 1000 ms after the cue. The 200 ms period prior to onset was used for baseline correction. All single trial EMG clench traces are displayed in Figure 2.

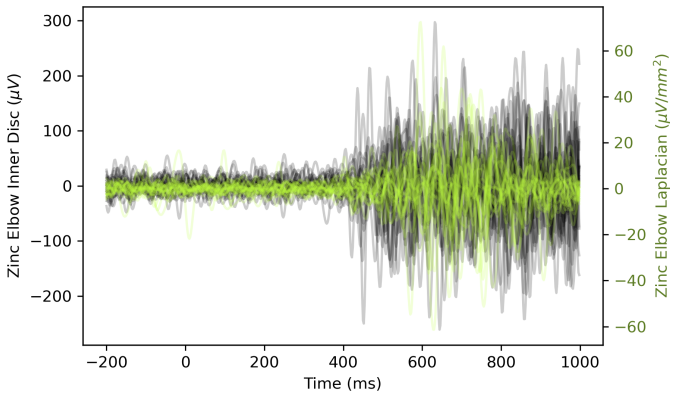

Fig. 2. EMG Clench Epochs. 25 trials of EMG data from zinc elbow inner disc (black) with 25 trials from zinc elbow Laplacian (green) overlaid.

To quantify signal quality, signal-to-noise ratio (SNR) was calculated for each epoch, across all four movements for hand inner disc, Laplacian hand, elbow inner disc, and Laplacian elbow for each metal type using:

$$\text{SNR (dB)} = 10\log_{10}\frac{\text{POWER}_{\text{SIGNAL}}}{\text{POWER}_{\text{NOISE}}} \tag{2}$$

Results are reported in decibels (dB) in Figure 4. Further SNR results for all four movements can be found in Table I. For all gestures, movement began roughly 400 ms after the display of the cue. Power of the noise was quantified in the -200 to 400 ms window for each epoch and the signal power was calculated in the 400 to 1000 ms range of each epoch. Note that when the signal is measured in this way, it includes the noise. However, if the intended use is the detection of movement by thresholding, a positive SNR (when measuring signal as above) should be sufficient.

III. Results

A. EIS

Given the comparison of the raw impedance data for all electrodes, it is seen that the zinc electrodes consistently outperform the stainless steel electrodes with a lower impedance at all frequencies. The zinc CRE performs approximately the same as the bleach fabricated electrode from [5] below 2 Hz, at which point the impedance of the zinc CRE is consistently below that of the bleach electrode. Both zinc electrodes have impedance below that of the bleach fabricated electrode above 2 Hz and perform better than the Ink Ag/AgCl electrode with a lower impedance above 15.9 Hz. From the comparison of the area-normalized impedance data for all electrodes, it is seen that the stainless steel electrodes still perform worse than

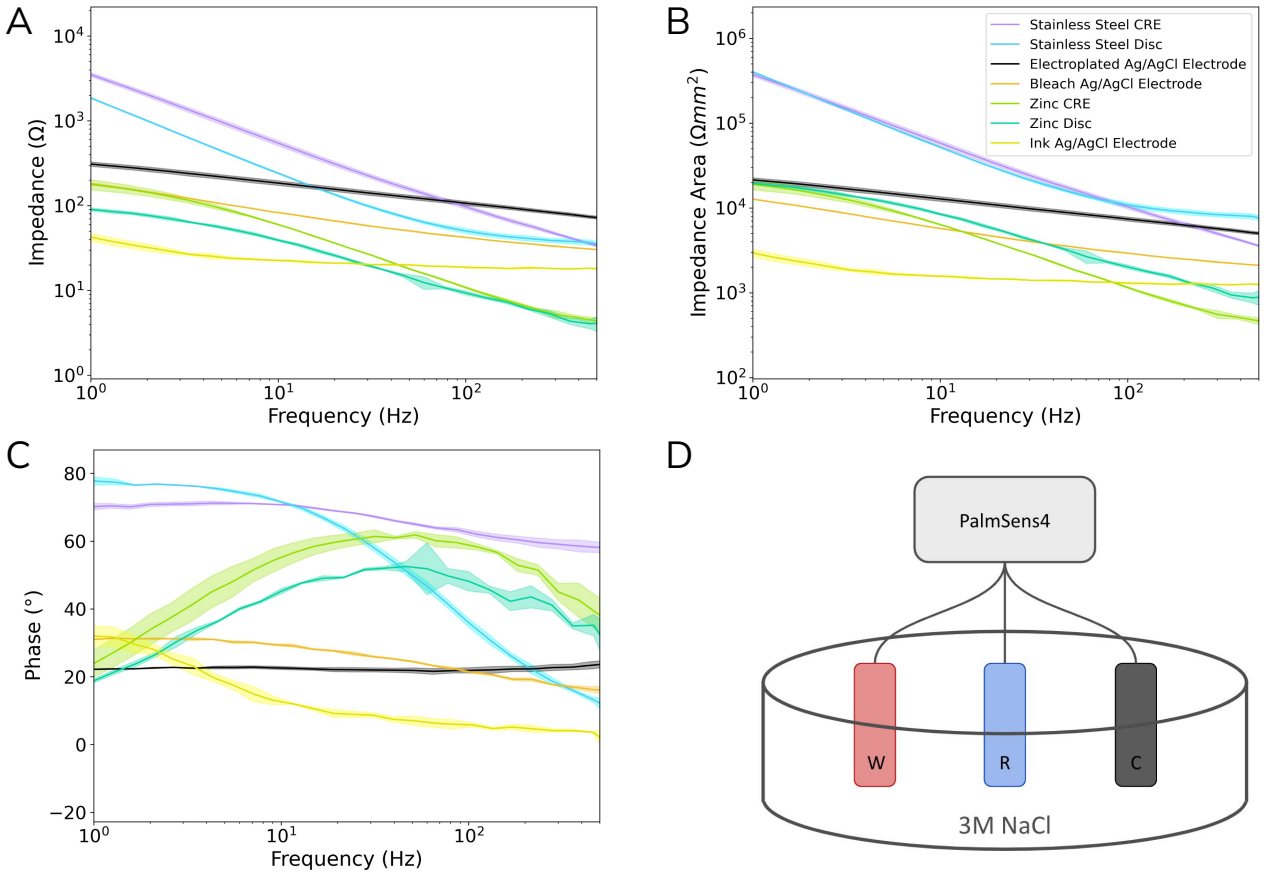

Fig. 3. EIS setup and results. (A) Average impedance vs. frequency of the electrodes fabricated in this paper and the best three electrodes from Lee et al. (B) The area normalized average impedance vs. frequency plot of the electrodes fabricated alongside the electrodes from Lee et al. (C) Average phase vs. frequency plot of all electrodes. (D) The EIS setup used for all zinc and stainless steel electrodes. W refers to working electrode, R refers to reference electrode, and C refers to counter electrode. The solution was 3M concentrated NaCl in deionized water.

the rest with the highest impedance. The zinc electrodes also performed worse than both the bleach and ink electrodes with higher impedance at lower frequencies, but better than the electroplated electrode with lower impedance at frequencies above 2 Hz.

B. EMG

SNR data for clenches recorded from elbow channels are displayed in Figure 4. SNR was found to be around 13 dB for both zinc elbow inner disc and zinc elbow Laplacian, with greater standard deviation in the Laplacian (5.3) than the inner disc (2.5). For all stainless steel electrodes, no significant difference was observed between the signal power before and after movement. The results for electrodes closer to the hand are comparable. SNR data for all movement tasks are reported in I.

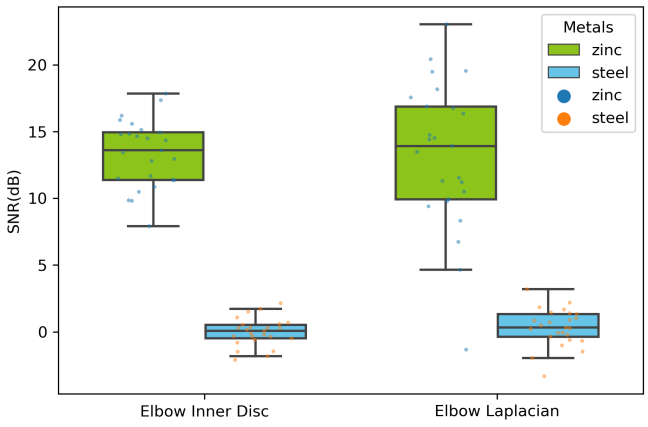

Fig. 4. SNR Boxplots. Distribution of single trial SNR values from zinc elbow inner disc and zinc elbow Laplacian, compared with stainless steel electrode recordings.

IV. Discussion

Overall, stainless steel was not found to be a high quality electrode, as expected, however zinc had low characteristic impedance and high enough SNR to be useful in monitoring muscle activity. Tripolar concentric ring electrodes, with Laplacian re-referencing has been shown to increase spacial resolution of EMG recordings [11]. However, we did

TABLE I
SNR COMPARISON TABLE. SNR VALUES ACROSS ALL MOVEMENT CONDITIONS, COMPARING ZINC VS. STAINLESS STEEL AND INNER DISC ELECTRODES VS. CRES WITH LAPLACIAN FILTERING. ALL VALUES ARE IN DECIBELS. VALUES IN PARENTHESES ARE STANDARD DEVIATIONS.

	Clench	**Up**	**Down**	**Expand**
Zinc Elbow Laplacian	13.25 (± 5.36)	12.58 (± 3.696)	12.28 (± 3.82)	10.71 (± 4.218)
Zinc Elbow Inner Disk	13.34 (± 2.472)	8.477 (± 2.297)	8.553 (± 2.891)	11.66 (± 2.62)
Steel Elbow Laplacian	0.3226 (± 1.37)	0.08366 (± 1.2)	-0.2538 (± 1.511)	-0.2396 (± 1.448)
Steel Elbow Inner Disk	-0.01509 (± 1.024)	-0.1215 (± 1.145)	-0.1504 (± 0.99)	0.1129 (± 1.235)

not observe increased signal quality in the concentric ring arrangement over the inner disc. It is possible that the electrode placements and use cases were not optimally chosen to get the most benefit out of CREs and observe the increased spatial resolution.

A. EIS

Conclusions about the performance of the fabricated electrodes as a whole can be made by analyzing the raw impedance data from Figure 3. This allows for the electrodes to be considered as an entire unit, rather than just the impedance of the material or arrangement individually. By assessing impedance values (lower is preferable), the zinc electrodes outperform the ink electrodes above 15.9 Hz, and outperform the bleach electrodes at frequencies above 2 Hz. The zinc discs outperform the bleach fabricated electrodes at all frequencies. The area-normalized impedance graphs also show that as a material, zinc outperforms Ag/AgCl electrode material fabricated by electroplating. Together, these results suggest that zinc may be viable for electrophysiological recording. Small differences might be observed if the Ag/AgCl recordings were performed concurrently with the zinc and stainless steel electrodes.

B. EMG

Results show that zinc's SNR is high enough to detect various hand movements. However, there was no observed benefit with the tripolar concentric ring arrangement, as the SNR variance was higher in both hand and elbow electrodes. It remains to be seen whether the tripolar concentric ring layout can improve signal quality and spatial resolution when electrolytic gel is applied, leading to a consistent bridge between the skin and all three of the electrodes. More research into the effects of zinc electrodes on skin is required, such as its toxicity and reactivity. The zinc-skin interface also needs to be studied as electrode-skin interfaces are known to be complex within the commonly studied EMG frequency range [7]. Finally, systematic comparisons must be conducted with simultaneous Ag/AgCl and zinc recordings to demonstrate zinc is a suitable replacement in real-world applications.

ACKNOWLEDGMENT

CR, AD, and MSL performed EIS; CR, AD, AT, and JF performed EMG recordings. EIS data were analyzed by CR, EMG data were analyzed by AT and JF. JHK, MSL, and GC assisted with EIS theory, while VdS assisted with electrophysiology theory and analysis. CR, AD, AT, JF and VdS wrote and edited paper. This project was funded by HDSI Data Planet Fellowship awarded to AD, an NSF REU awarded to CR, AT, and JF under VdS (NSF awards #1817226 and #2335645) and an HDSI Undergraduate Scholarship awarded to AT and JF, which also supported their graduate supervisor AD. Silver EIS data provided by MSL. We would like to thank UCSD's Makerspace for assisting in the fabrication of the electrodes. The authors report no conflicts of interest.

REFERENCES

[1] Brain Vision, LLC; Brain Products GmbH, *BrainAmp*. [Online]. Available: https://www.brainproducts.com/solutions/brainamp/.

[2] *BrainAmp series LSL connector*. [Online]. Available: https://github.com/brain-products/LSL-BrainAmpSeries.

[3] G. Di Flumeri, P. Aricò, G. Borghini, N. Sciaraffa, A. Di Florio, and F. Babiloni, "The dry revolution: Evaluation of three different eeg dry electrode types in terms of signal spectral features, mental states classification and usability," *Sensors*, vol. 19, no. 6, p. 1365, 2019.

[4] C. Kothe, *Lab Streaming Layer (LSL)*, 2014. [Online]. Available: https://labstreaminglayer.org.

[5] M. S. Lee, A. Paul, Y. Xu, W. D. Hairston, and G. Cauwenberghs, "Characterization of ag/agcl dry electrodes for wearable electrophysiological sensing," *Frontiers in Electronics*, vol. 2, p. 700 363, 2022.

[6] J. Linietsky, A. Manzur, and Godot Engine Contributors, *Godot Engine, 4.1*, 2023. [Online]. Available: https://docs.godotengine.org/en/4.1/.

[7] R. Merletti and P. Parker, *Surface electromyography: physiology, engineering, and applications*. John Wiley & Sons, 2004.

[8] PalmSens, *PSTrace version 5.8*, 2019. [Online]. Available: https://www.palmsens.com/.

[9] T. Stenner, C. Boulay, J. Hwang, *et al.*, *LabRecorder*. [Online]. Available: https://github.com/labstreaminglayer/App-LabRecorder.

[10] P. Virtanen, R. Gommers, T. E. Oliphant, *et al.*, "SciPy 1.0: Fundamental Algorithms for Scientific Computing in Python," *Nature Methods*, vol. 17, pp. 261–272, 2020. DOI: 10.1038/s41592-019-0686-2.

[11] K. Wang, U. Parekh, T. Pailla, H. Garudadri, V. Gilja, and T. N. Ng, "Stretchable dry electrodes with concentric ring geometry for enhancing spatial resolution in electrophysiology," *Advanced healthcare materials*, vol. 6, no. 19, p. 1 700 552, 2017.